Experimental Investigation of Phase-Space Portraits of Ideal Four-Wave Mixing

Anastasiia Sheveleva, Andrei V Ermolaev, Pierre Colman, J.M. M Dudley, Christophe Finot

Experimental Investigation of Phase-Space Portraits of Ideal Four-Wave Mixing

Anastasiia Sheveleva [1,*], Andrei Ermolaev [2], Pierre Colman [1], John M. Dudley [2], Christophe Finot [1]

[1] *Laboratoire Intersdisciplinaire CARNOT de Bourgogne, UMR 6303 CNRS-Université de Bourgogne, Dijon, France*

[2] *Université de Franche-Comté, Institut FEMTO-ST, CNRS UMR 6174, Besançon, France*

Tel: (+33) 380395926, Fax: -, e-mail: anastasiia.sheveleva@u-bourgogne.fr

ABSTRACT

We develop a fiber-based experimental setup dedicated to the demonstration of an ideal four-wave mixing process. With an experimental technique based on the iteration of initial conditions and propagation over short distances of fibers, we are able to alleviate the impact of high-order harmonics and optical losses. We can therefore mimics nearly ideal propagation over tens of kilometers and reveal the complete phase-space topology exhibiting several Fermi-Pasta-Ulam-Tsingou recurrence cycles, the existence of a stationary wave as well as the presence of a system separatrix, which marks the transition between two distinct spatiotemporal evolution regimes. The experimental dynamics agrees well the theoretical predictions with close orbits that do not intersect.

We also investigate theoretically and experimentally an impact of control parameters on orbits' dynamics. We use an abrupt change in power to connect two states on the phase-space plane that do not belong to the same trajectory. Finally, we apply machine learning techniques: firstly, we train a feed-forward neural network with non-iterated sampled measurements that allows to extract the key characteristics of the dynamics; and secondly, we use a sparce identification of nonlinear dynamics to retrieve differential equations governing the four-wave mixing dynamics affected by noise.

Keywords: nonlinear fiber optics, experiment, four-wave mixing, modulation instability, Fermi-Pasta-Ulam recurrence, machine learning.

1. INTRODUCTION

The nonlinear Schrodinger equation (NLSE) governs wave evolution in many nonlinear systems such as fiber optics, hydrodynamics, plasma physics, Bose-Einstein condensates, and others [1], where the wave undergoes changes in a dispersive medium with an intensity-dependent nonlinear shift. The key process underlying the wave dynamics is the four-wave mixing (FWM), which can be described as an energy exchange between discrete frequency components under impact of both dispersion and nonlinearity. The FWM effect is the most pronounced in the degenerate case when a single pump generates sidebands with upshifted and downshifted frequencies. If the interaction is reduced to only three spectral lines (the pump and two sidebands), the NLSE evolution can be simplified to a set of three differential equations, that can be associated to a conservative Hamiltonian system. This fundamental FWM is experimentally tricky to be rigorously demonstrated due to the fast growth of residual spectral lines that are generated through cascaded interactions [2], where the newly appeared sidebands act as pumps themselves triggering further energy exchange. However, the ideal FWM at its three-waves limit remains an interesting problem for experimental demonstration.

2. IDEALIZED FOUR-WAVE MIXING DEMONSTRATION

2.1 Theoretical background

First, we give a small reminder of the ideal FWM dynamics. Assuming a lossless propagation in a single-mode fiber, the slowly-varying electric field envelope $\psi(z,t)$ is governed by the NLSE :

$$i\frac{\partial \psi}{\partial z} - \frac{\beta_2}{2}\frac{\partial^2 \psi}{\partial t^2} + \gamma |\psi|^2 \psi = 0, \qquad (1)$$

where z is the propagation distance, and t is a time in a reference frame. The β_2 denotes the second-order dispersion coefficient (here, the anomalous dispersion is considered, so $\beta_2 < 0$), and γ is the nonlinear Kerr coefficient. If one assumes an interaction solely between the pump and two lines at $\pm\omega_m$ (with $\omega_m = 2\pi f_m$ being the modulation frequency), the total electric field reads as: $\psi(z,t) = \psi_0(z) + \psi_{-1}(z)\exp(i\omega_m t) + \psi_1(z)\exp(-i\omega_m t)$. Note that here we consider the focusing NLSE case, therefore a mismatch parameter for the spectral lines within the modulation instability gain is $\Omega^2 = sign(\beta_2)(2\pi f_m)^2/(|\beta_2|/\gamma P_0)$ with P_0 being the average power. Injecting the total field expression to Eq. (1), one receives a set of three coupled differential equations that were extensively studied in [3], and are referred to as an ideal FWM system. This system can be equivalently described in terms of the one-dimensional conservative Hamiltonian :

$$H = 2\eta(1-\eta)\cos\phi + (\Omega^2+1)\eta - \frac{3}{2}\eta^2, \qquad (2)$$

where $\eta = |\psi_0|^2 / \sum|\psi_i|^2$ is the relative spectral amplitude and $\phi = \phi_{-1} + \phi_1 - 2\phi_0$ is the relative phase with ϕ_i being the phase of each spectral line. The energy exchange between the lines along the propagation length is governed by the following equations, where ξ -is the normalized distance $\xi = z\,(\gamma P_0)$:

$$\frac{\partial \eta}{\partial \xi} = \frac{\partial H}{\partial \phi} \quad \text{and} \quad \frac{\partial \phi}{\partial \xi} = -\frac{\partial H}{\partial \eta}. \tag{3}$$

Using the notations developed above, the change in amplitude and phase between three spectral lines reveals a recursive nature of the dynamics : if the process starts with a strong pump, the energy first is redistributed between the sidebands, but then flows back to the pump. This phenomenon is referred to as Fermi-Pasta-Ulam (FPU) recurrence. A convenient way to study the evolution is to use a phase-space plane with ($\eta\cos\phi$, $\eta\sin\phi$) coordinates. The exact dynamic of wave propagation depends on initial relative phases and amplitudes, hence one observes different types of orbits (black dashed lines in Fig. 1(b)) that can be assigned to two types of solution divided by a separatrix : ones with bounded phase on the right, and others with unbounded phase on the left [4].

2.2 Experimental setup and dynamics reconstruction

Up to date the FPU recurrence and FWM dynamics were experimentally demonstrated for the cascaded FWM system, where the generation of residual spectral lines was not restrained [3,4]. Even though these results reveal FPU recurrence cycles, a demonstration of the ideal FWM over an entire phase-space plane has remained unaddressed.

To demonstrate the ideal FWM the setup depicted in Fig. 1(a) has been developed [5]. We start with a continuous wave (CW) laser (at 1550 nm) which is modulated by the phase modulator (PM) to generate a spectral comb (at 40 GHz), which is then shaped by the programmable spectral filter to match the initial η, ϕ. The three spectral lines are amplified to reach the average power level P_0, then they propagate in a short segment of a single-mode fiber (β_2 = -8 ps^2 km^{-1} ; γ = 1.7 W^{-1} km^{-1}). If the fiber is sufficiently short, 500 m length in our case, the residual spectral lines will not develop, therefore the ideal FWM model remains valid. The next stage is the measurement of the changes in spectral amplitude and phase induced by propagation in the fiber : the spectral amplitudes are measured directly with the optical spectrum analyser (OSA), and the spectral phase is retrieved from a relative beating between two sinusoidal waves that result from filtering out the $\pm f_m$ components. The output values are then gathered by a computer that then automatically updates the input values, and the process is repeated in a loop. With such a continuous update of initial conditions the dynamics can be reconstructed over several tens of kilometres and include several recurrence cycles.

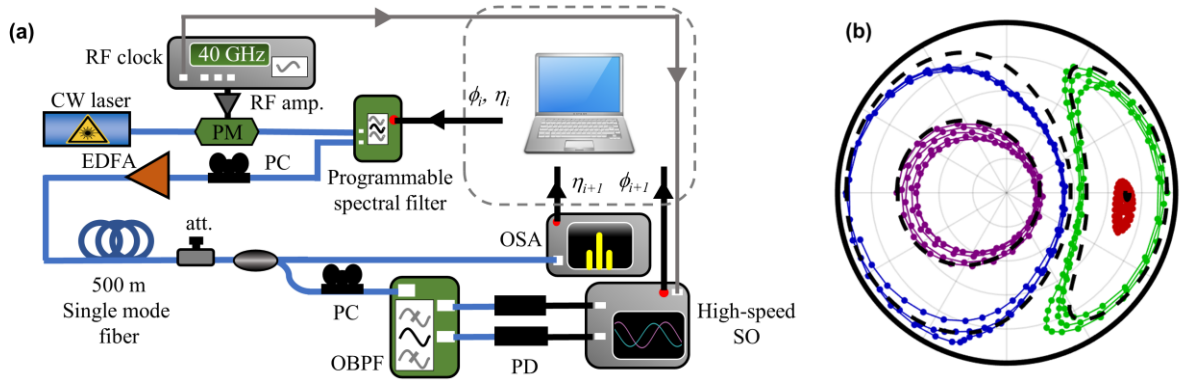

Figure 1 (a) Experimental setup : PC – polarisation controller; EDFA – erbium-doped fiber amplifier; OBPF – optical band-pass filter; PD – photodiode; high-speed SO – high-speed sampling oscilloscope. (b) Results of the measurements depicting evolution of (η,ϕ) on the phase-plane for input relative amplitudes of 0.95, 0.70 for phase of π and 0.95, 0.65 for the phase of 0 radians (blue, purple, green and red lines, respectively).

Figure 1 (b) displays the measured FWM dynamics for several initial conditions (at P_0 = 21.7 dBm = 150 mW, hence Ω^2 = -2) over 50 km (100 iterations). The evolution follows closely the one predicted by the ideal model, and the recurrence is revealed, while two types of trajectories are well separated. The discrepancies are attributed to experimental errors accumulated due to iterations and small deviations from the ideal model.

3. TRAJECTORIES CONTROL

The normalized mismatch parameter Ω in Eq. (2) can be interpreted as a control parameter of the system [6]: indeed, depending on Ω the orbits shapes and position of the separatrix would differ. Hence, using variation in Ω (for instance, change in fiber parameters or in the input average power), one can control the dynamic, and make

a transition from one state to another. If there is no limit in reachable values of Ω, one can connect any two points on the diagram with a single transition. However, when the experimental limitations are introduced: in our case, fixed fiber parameters and power limits, the range becomes limited to Ω^2 = [-2.51 : -0.95]. Using the conservation of the Hamiltonian (Eq. (2)) we derive a range of points on the map that are reachable withing the given limits imposed on Ω for both (η_{IN}, ϕ_{IN}) and (η_{OUT}, ϕ_{OUT}) to be connected. Then we find the best intersection point that is defined as the shortest distance (first, because we want to have the "fastest" connection, and second, because it allows to accumulate less errors).

Experimentally the trajectories control is realized by implementing an abrupt change in the average power P_0 that is adjusted by the EDFA. In Fig. 2(a) and (b) two points that do not belong to the same trajectory are connected by controlling the power. This approach allows to connect points located either on the opposite or on the same sides of the separatrix.

Overall, we demonstrate as the input average power can be used as a control parameter, hence as a degree of freedom, allowing tailored control of dynamics in the ideal FWM system [7].

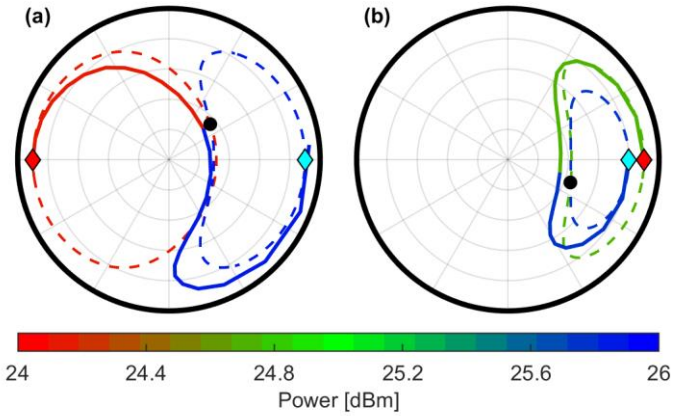

Figure 2 Experimental trajectories that connect (a) η_{IN} = 0.90, ϕ_{IN} = π and η_{OUT} = 0.90, ϕ_{OUT} = 0, (b) η_{IN} = 0.90, ϕ_{IN} = 0 and η_{OUT} = 0.80, ϕ_{OUT} = 0, by an abrupt power change. The colour depicts value of input average power that is used for each part of the trajectory.

4. MACHINE LEARNING APPLICATIONS

As it was demonstrated in the previous sections, the dynamics follows closely the ideal FWM evolution, however it's still impaired by experimental inaccuracies and fundamental differences related to generation of small residual sidebands. Hence, a question of noise impact and uncharacterized experimental effects remains open. To characterize the system, we use the machine learning applications: first, we train a neural network on the experimental data, and second, we apply the Sparce Identification of Nonlinear Dynamics (SINDy) technique to conclude on how the ideal model can be impaired by random noise.

4.1 Neural Network reconstruction

The machine learning strategies, namely the neural networks (NN), have boosted many aspects of photonics and nonlinear fiber optics [8]. Here we train a simple feed-forward NN on the experimental data to construct an emulator of the experiment disposable at hand, that would allow to get the data for arbitrary input conditions.

The selected NN's structure is composed of three layers with 12 neurons in total (Fig. 2(b)), where the input parameters are power and positions on the phase-space diagram. The output of the NN predicts a result of propagation over a segment of fiber. The training data consists of 1800 points randomly sampled points on the map at discrete powers [21.8 : 0.5 : 24.3] dBm (Fig. 3(a)). In the result of the training the mean-square error of 2.54×10^{-4} is achieved allowing precise reconstruction of the dynamics with experimental features included. Even though the NN was trained on discrete set of points, it can reconstruct the closed orbits characteristic of the ideal FWM (Fig. 3 (c)) and interpolate the dynamics for the powers not included in the training set [9].

4.2 Sparce identification of nonlinear dynamics

The SINDy is a data-driven approach that aims in finding the smallest number of terms from a library of functions that can reproduce the dynamics in terms of differential equations [10]. This technique was applied to reconstruct Eq. (3) from 20 trajectories generated by the ideal FWM equations (with random initial conditions at fixed Ω) that were impaired by 2.5-7.5% noise [11]. The results demonstrate that the exact FWM equations can

be retrieved with good accuracy and robustness even from the noisy data. Therefore, one may anticipate implementation if this technique to a system, where the underlying model is not known in advance, or on the experimental results strongly impaired by an unknown phenomenon.

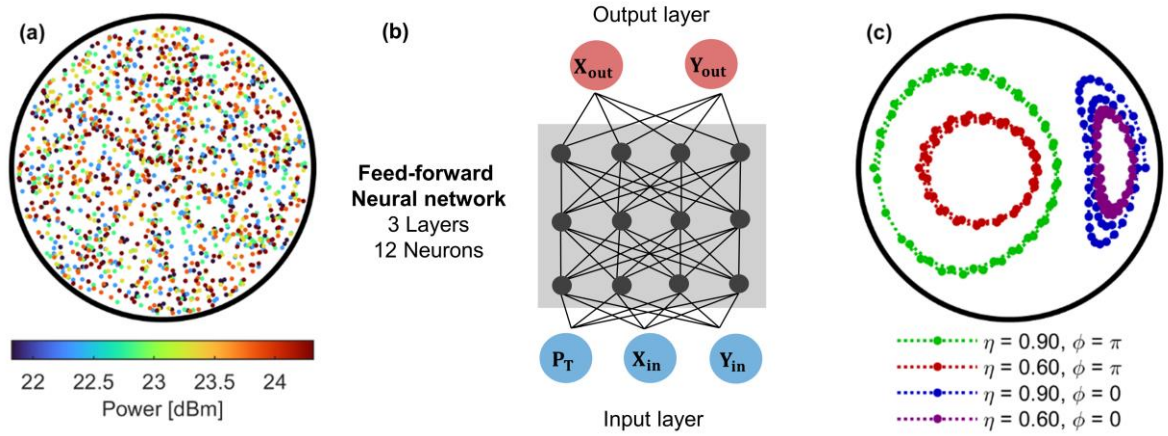

Figure 3 (a) Training data set : randomly selected points on the experimental map at different values of power from 21.8 dBm to 24.3 dBm. (b) Structure of the neural network (NN). (c) Trajectories resulting from the NN trained on the experimental data.

5. CONCLUSIONS

We demonstrate an ideal FWM dynamics with a novel experimental technique based on iteration of initial conditions. The input average power is used as a control parameter to connect two points that do not belong to the same trajectory. Finally, the machine learning techniques are used to reconstruct the complete dynamics in presence of noise and/or experimental deviations.

Our study fills in a gap of experimental demonstration of the fundamental process underlying the NLSE. The setup can be used for investigation of more complex systems such as non-degenerate FWM, parametric instability, normal dispersion propagation, or for more tailored types of control such as, for instance, the adiabatic transition between two states.

FUNDINGS

OPTIMAL (ANR-20-CE30-0004); Région Bourgogne-Franche-Comté; Institut Universitaire de France; CNRS (MITI interdisciplinary programs).

REFERENCES

[1] C. Sulem and P.L. Sulem: The nonlinear Schrödinger equation: self-focusing and wave collapse, *Springer Science & Business Media*, Vol. 139, 2007.

[2] A. Mussot et al.: Fibre multi-wave mixing combs reveal the broken symmetry of Fermi–Pasta–Ulam recurrence, *Nat. Photon*. 12, 303-308, 2018.

[3] G. Cappellini and S. Trillo: Third-order three-wave mixing in single-mode fibers: exact solutions and spatial instability effects, *J. Opt. Soc. Am. B* 8, 824-838, 1991.

[4] C. Naveau, P. Szriftgiser, A. Kudlinski, M. Conforti, S. Trillo, and A. Mussot: Full-field characterization of breather dynamics over the whole length of an optical fiber. *Opt. Lett*., 44(4):763–766, Feb 2019.

[5] A. Sheveleva, U. Andral, B. Kibler, P. Colman, J. M. Dudley, and C. Finot: Idealized four-wave mixing dynamics in a nonlinear Schrödinger equation fiber system, Optica 9, 656-662, 2022.

[6] Z. Deng, J. Zhang, D. Fan, and L. Zhang: Manipulation of breather waves with split-dispersion cascaded fibers, *New J. Phys*. 24, 063018, 2022.

[7] A. Sheveleva, P. Colman, J.M. Dudley, C. Finot : Trajectory control in idealized four-wave mixing processes in optical fiber. Optics Communications, in press, 2023, arXiv:2303.08469 .

[8] G. Genty et al.: Machine learning and applications in ultrafast photonics, *Nat. Photon*. 15, 91-101, 2021.

[9] A. Sheveleva, P. Colman, J. M. Dudley, and C. Finot: Phase space topology of four-wave mixing reconstructed by a neural network, *Opt. Lett.* 47, 6317-6320, 2022.

[10] S.L. Brunton, J.L. Proctor, and J.N. Kutz: Discovering governing equations from data by sparse identification of nonlinear dynamical systems, *Proc. Natl. Acad. Sci.*, 113, 3932–3937, 2016.

[11] A. V. Ermolaev, A. Sheveleva, G. Genty, G. et al.: Data-driven model discovery of ideal four-wave mixing in nonlinear fibre optics, *Sci Rep*, 12, 12711, 2022.